Synthesis, structure and film-forming properties of poly(butyl methacrylate)–poly(methacrylic acid) core–shell latex

Haeng-Boo Kim*, Yongcai Wang† and Mitchell A. Winnik‡
Department of Chemistry, University of Toronto, Toronto, Ontario M5S 1A1, Canada
(Received 20 December 1992; revised 8 July 1993)

The preparation and characterization are described of a series of core–shell poly(butyl methacrylate) latex particles containing varying amounts of carboxylic acid groups. Matched pairs of particles, labelled with either donor (phenanthrene) or acceptor (anthracene) groups, were prepared by three-stage emulsion polymerization under monomer-starved conditions in which varying amounts of methacrylic acid were introduced into the third-stage polymerization. Films were prepared from the latex. The rate of polymer interdiffusion in the films, as followed by energy transfer measurements, decreased as the carboxyl content of the latex shell increased.

(Keywords: poly(butyl methacrylate); poly(methacrylic acid); core–shell latex)

INTRODUCTION

One of the features of latex film formation that makes it different from other polymer-welding processes[1,2], such as the sintering of polymer powders[3], is the presence of hydrophilic material at the latex particle surface. If the amount of hydrophilic material is sufficient, it may form a membrane during the film formation process. These membranes have been detected in transmission electron microscopy (TEM) through staining of thin sections obtained through cryoultramicrotoming[4–9], and they have been inferred from small-angle neutron-scattering (SANS) experiments in which D_2O is allowed to sorb into previously dried latex films[7–9].

It has been suggested that this membrane can act as a barrier to interparticle polymer diffusion[4–9]. This interdiffusion is normally responsible for the growth in strength accompanying the healing of the interface in a polymer weld[1,2]. If polymer interdiffusion is restricted or prevented, then it is possible that another mechanism is responsible for the mechanical strength of such latex films.

One way to examine the effect of hydrophilic surface layers on latex films is to study directly the polymer interdiffusion process in films prepared from a series of latex particles in which the surface structure is varied systematically. Polymer interdiffusion can be studied by SANS[3,10–13] or by fluorescence spectroscopy using direct non-radiative energy transfer (DET) measurements[14–17]. Both techniques require labelled polymers, ^2H labelling for SANS, and fluorescent labelling for DET. To study the influence of surface structure on interdiffusion in latex films, one must be able to vary the structure of the particle surface in the context of synthesizing a series of latex particles.

In this paper we describe the application of the DET method to the study of interdiffusion in a series of poly(butyl methacrylate) (PBMA) latex particles containing differing amounts of carboxylic acid groups at the surface. These particles are prepared by three-stage semicontinuous emulsion polymerization in which varying amounts of methacrylic acid (MAA) are mixed with butyl methacrylate (BMA) in the final stage of the synthesis. Here we report the synthesis and characterization of the latex particles as well as initial studies of the influence of surface structure on polymer interdiffusion in annealed latex films.

EXPERIMENTAL

Materials

9-Anthryl methacrylate (AnMA) and 9-phenanthrylmethyl methacrylate (PheMMA) were the same samples as employed previously[14–17]. Butyl methacrylate (BMA) and methacrylic acid (MAA) were distilled under vacuum just prior to use. Potassium persulfate (KPS), sodium bicarbonate and sodium dodecylsulfate (SDS, Aldrich) were used as received. Water was Milli-Q™ grade.

Emulsion polymerization

All particles used in this study were prepared from a single batch of unlabelled PBMA seed latex of diameter $d = 80$ nm. Recipes are presented in *Table 1*. To an aliquot of seed latex in water at 80°C were added initiator and surfactant in water and BMA plus fluorescent monomer simultaneously into the solution under monomer-starved conditions (1 ml h^{-1}). In this way we prepared the two samples An-MA0 and Phe-MA0. Samples of An-MA0 and Phe-MA0 were subsequently used as seeds for the preparation of the pairs of samples MA2, MA4 and MA6. In this third stage, additional surfactant and initiator in water were added slowly to the reaction (1 ml h^{-1}) while at the same time adding additional fluorescent monomer

* Permanent address: Department of Chemistry, Faculty of Engineering, Hokkaido University, Sapporo 060, Japan
† Permanent address: Eastman Kodak Co., Building 46, 2nd Floor, Room 222, Research Park, Rochester, NY 14650, USA
‡ To whom correspondence should be addressed

0032-3861/94/08/1779–08

Table 1 Emulsion polymerization recipe and conditions

Seed		Second stage (MA0)		Third stage (MA*x*)	
				MA0	20.0 ml
				Water	5.0 ml
Water	45.0 ml	Water	20.0 ml	Water	4.0 ml
BMA	3.25 ml	KPS	0.0361 g	KPS	0.0075 g
KPS	0.0428 g	SDS	0.47 g	SDS	0.05 g
SDS	0.0810 g				
$NaHCO_3$	0.0816 g	BMA	24.0 ml	BMA + MAA[a]	4.33 g
		AnMA	0.393 g or	AnMA	0.0698 g or
		PheMMA	0.446 g	PheMMA	0.0793 g
Temperature	80°C	Temperature	80°C	Temperature	80°C
Time	1 h	Time	22 h	Time	20 h

[a] 0.0528 g MAA + 4.275 g BMA for MA2, 0.1065 g + 4.221 g for MA4 and 0.2500 g + 4.077 g for MA6

dissolved in the appropriate mixture of BMA and MAA. We did not monitor monomer consumption until the end of the reaction. The long reaction times (ca. 20 h, *Table 1*) reflect experimental convenience rather than some intrinsic requirement of the reaction itself.

Ion-exchange cleaning

To remove surfactant and other water-soluble ionic materials from the latex, ion-exchange cleaning was carried out. Ion-exchange resin (Biorad, AG-501-X8 mixed bed resin) was washed with hot deionized water (> 80°C), methanol and then deionized water before use. Twice the weight of the resin, based upon latex solids, was added to the diluted latex dispersion (solids content about 1 wt%) and then the mixture was stirred at room temperature for 30 min. The resin was removed by slow, gentle vacuum filtration. The process was repeated more than three times. Finally, the latex dispersion was concentrated up to 20 wt% solids content by using a rotary evaporator.

Characterization

The latex particle sizes were measured by the dynamic light-scattering technique (Brookhaven Instruments BI-90 particle sizer). The molecular weights were determined by gel permeation chromatography (g.p.c.) (Waters Microstyragel columns, THF as eluent, monodisperse poly(methyl methacrylate) samples as standards). Surface charge densities were determined by potentiometric titration under a nitrogen atmosphere. The freshly ion-exchanged latex was titrated directly ('forward titration') with aqueous NaOH (6.01×10^{-3} M). After addition of an excess amount of aqueous NaOH (to pH 12.5), reverse titration with aqueous HCl (0.167 M) was carried out. Typical examples of the titration curves are shown in *Figure 1*. The latex was dried and then dissolved in THF. The solution was then titrated with sodium methoxide in methanol, the result of which gave the bulk charge density of acid (sulfuric and carboxylic acid which exist both on the surface and inside the particle) Q_b.

Film formation and annealing

A few drops of a dispersion containing equal amounts of Phe-labelled and An-labelled latex were placed on a small quartz plate (ca. 5 × 10 mm) previously warmed on a hotplate to 32°C. A petri dish was inverted over the film to slow down the drying process. Drying occurred over a period of ca. 4 h to yield transparent and void-free films 30–50 μm thick. Fluorescence decay measurements were carried out on these films prior to annealing them in an oven at 90°C. To anneal films for short periods of

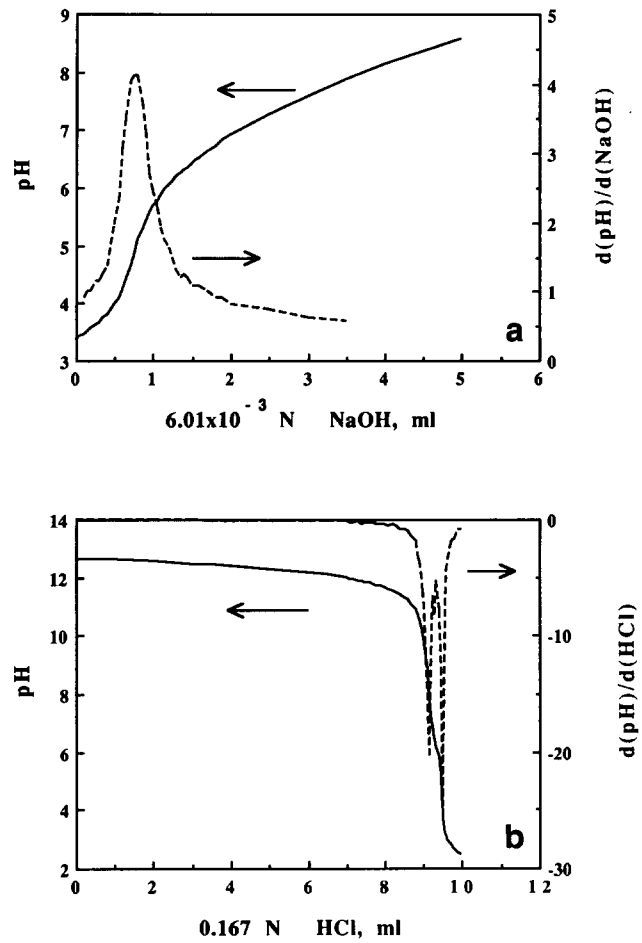

Figure 1 Potentiometric titration curves for an aliquot of latex An-MA4, including first-derivative plots (dashed lines) of the data: (a) forward titration with 6.01×10^{-3} M NaOH; (b) after raising the pH to 12.5 with excess NaOH, reverse titration with 0.167 M HCl. For these titrations we used 5.482 g of the Phe-MA4 dispersion with 18.7 wt% solids

time, the quartz substrates supporting the films were placed directly on a high-mass aluminium slab inside a convection oven prewarmed to 90 ± 1°C. For films annealed for longer periods of time, steps were taken to prevent film and chromophore oxidation. The films were placed inside small test tubes which were sealed with a septum. Using flowing gas and syringe needles, an argon atmosphere was introduced to the test tube, and the test tube was placed in the oven at 90°C. Samples were removed from the oven and cooled to room temperature for fluorescence measurements.

Samples for fluorescence decay measurements were placed in a small quartz test tube under an argon atmosphere. Decay profile measurements were carried out using the single-photon timing technique as described previously[14–17]. Phenanthrene decay profiles $I_D(t)$ were monitored at 366 nm, with $\lambda_{ex} = 300$ nm.

RESULTS AND DISCUSSION

Latex synthesis

In these experiments we wished to produce a series of latex pairs, one component labelled with phenanthrene (Phe), the other labelled with anthracene (An), the components of which were similar in size, molecular weight and molecular weight distribution, but differ only in the content of carboxyl groups. To simplify the synthesis, we began with the preparation of an unlabelled PBMA seed latex which was subsequently employed in the synthesis of both the Phe-labelled and An-labelled latexes. The second-stage polymerization, with slow, continuous feed of both the aqueous components (SDS, initiator) and the monomer mixture (BMA plus PheMMA or AnMA), yielded two samples of labelled latex, Phe-MA0 and An-MA0. These dispersions, at this point essentially identical to those employed in our previous studies, are stabilized in a colloidal sense only by sulfate groups on the surface. There are two sources of sulfate groups, those originating from the persulfate initiator and chemically bound to a chain end, and those from the SDS surfactant.

Using the two MA0 samples as seeds, a third-stage emulsion polymerization was carried out to introduce carboxylate groups into the particles. In the third stage, the chromophore content was matched to that of the second stage, but MAA was included with BMA in the feed. The ratio of MAA to BMA was increased in preparing MA2, MA4 and MA6. Particle sizes are listed in *Table 2*. The carboxylated latex particles were 20 nm larger in diameter than the MA0 seed. The mean volume for MA0 is 1.13×10^6 nm^3 per particle, whereas for MA2 to MA6 it is 1.75×10^6 nm^3 per particle. Thus, the carboxylated copolymer represents approximately 35 vol% of the polymer in the particle.

Particle characterization

The particles prepared are completely soluble in organic solvents like chloroform, ethyl acetate and THF, and thus have no detectable gel content. Size exclusion chromatography (s.e.c.) in THF in conjunction with dual detectors allows the molecular weight to be estimated (relative to PMMA standards) and the molecular weight distribution to be determined. Values are presented in *Table 2*. Values of both M_w and M_w/M_n are very similar for all samples. The ultra-violet detector indicated that more than 99% of the chromophore is attached to the polymer.

Surface charge was titrated potentiometrically. Because bulk pH is not simply related to hydrogen ion activity at the particle surface, we cannot distinguish the titration of OSO_3H and CO_2H groups from the solution pH alone. Forward titration of the freshly ion-exchanged latex (*Figure 1*) titrates those groups immediately accessible on the surface of the particle. The forward titration values for surface charge (*Table 2*) are very small. Once the titration was complete (15 min), the pH was raised to 11. The particles were allowed to equilibrate for 20 min, and the dispersion was back titrated with HCl. There are two inflections in the reverse titration, which appear as two sharp peaks in the derivative plot (*Figure 1*). The high-pH inflection corresponds to titration of the excess NaOH, and that at pH ~4 corresponds to reprotonation of surface acid groups. A much larger number of acid groups is detected during the back titration than during the initial titration.

Such effects are very common in latex systems[18,19]. The most sensible explanation for the difference in equivalent acid groups in the reverse titration is that many groups are buried just beneath the surface. Upon exposure of the latex to base, these groups migrate to the surface on the timescale of several minutes and become neutralized. In support of this idea, we note a slow

Table 2 Characterization of carboxylated PBMA latexes

Sample	Particle size (nm)	$10^5 M_w$ (M_w/M_n)	Charge density[a] (10^{-5} eq g^{-1})			Actual parking area (Å^2 per acid)
			$Q_s(OSO_3H)$	$Q_s(CO_2H)$	Q_b	
An-MA0	129	4.8 (3.6)	1.0	0	3.5	730
Phe-MA0	128	4.1 (3.2)	0.99	0	3.2	750
An-MA2	152	4.8 (2.9)	0.52	4.0	8.4	140
Phe-MA2	147	4.4 (3.2)	0.58	4.4	8.8	130
An-MA4	150	4.2 (2.9)	0.48	7.5	12.2	79
Phe-MA4	150	4.0 (2.7)	0.44	6.1	11.7	96
An-MA6	149	4.9 (3.0)	0.42	11.2	26.0	55
Phe-MA6	146	4.3 (2.6)	0.48	11.6	27.1	54

[a] $Q_s(OSO_3H)$ and $Q_s(CO_2H)$ are the surface charge densities of sulfuric acid and carboxylic acid groups, respectively. Q_b is the bulk charge density of both acid groups

fall-off in pH with time immediately after raising the pH of the dispersion to 12. In the reverse titration, all of these now-exposed groups become protonated. When we refer to the surface acid concentration (Q_s in *Table 2*), we mean that quantity measured in the reverse titration. The total acid groups is determined by taking a weighed sample of freeze-dried latex, dissolving it in THF and titrating the solution with a previously standardized solution of sodium methoxide in methanol. This quantity of acid is referred to as Q_b in *Table 2*. Plots of Q_s and Q_b *versus* the mol% MAA in the third-stage feed are shown in *Figure 2*.

From these data we learn that a third of the OSO_3H groups in MA0 are in the surface region of the latex and approximately half of these are accessible only after neutralization. In the larger particles containing carboxylic acid groups, the number of groups detected in the forward titration (5×10^{-6} eq g^{-1}) is remarkably constant. The differences appear in both the 'subcutaneous' acid groups detected in the back titration and in the buried acid groups. These two quantities both increase approximately in proportion to the amount of MAA in the recipe.

The 'parking area' per acid group is calculated on the basis of the back titration results, and thus includes the groups just beneath the surface. The fraction of the surface occupied by acid groups in this series of particles spans a considerable range. If each acid group occupies ca. 25 Å^2, this fraction varies from 5% for MA0 to nearly 50% for MA6[20].

Data and data analysis

Fluorescence decay traces are presented in *Figure 3* for a film of MA4 annealed for various periods of time. In previous work[14–17] we have analysed these data in terms of a model predicated on the idea that we would decompose each decay trace into two contributions. An energy transfer contribution occurs from domains in the film where polymer diffusion has led to mixing of Phe and An groups. Superimposed upon this is an exponential decay contribution from Phe groups which have not yet mixed. These ideas lead to the expression

$$I_D(t) = B_1 \exp[(-t/\tau_D) - P(t/\tau_D)^{1/2}] + B_2 \exp(-t/\tau_D) \quad (1)$$

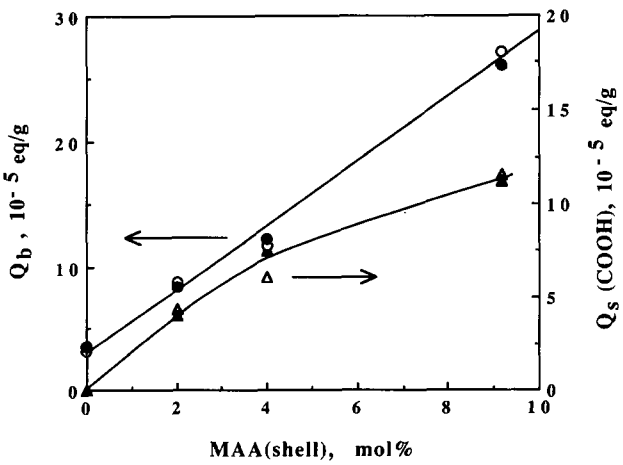

Figure 2 Plots of Q_s (titratable acid groups in the latex dispersion) and Q_b (total acid content of the latex) *versus* the mol% of MAA in the feed for the third stage of the emulsion polymerization: (○, △) Phe latex; (●, ▲) An latex

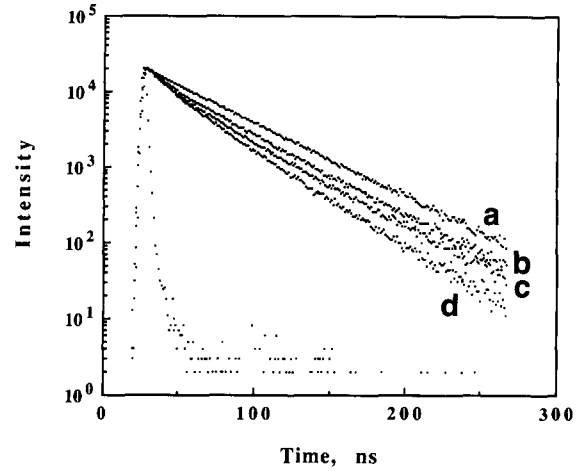

Figure 3 Fluorescence decay curves for a latex film composed of a 1:1 mixture of Phe-MA4 and An-MA4 for three different annealing times at 90°C: (a) as prepared; (b) 4 h; (c) 32 h. Also shown is the decay curve (d) from a solvent-cast film used to calculate $f'_m(\infty)$ and area(∞)

where the first term on the right-hand side in equation (1) is the energy transfer contribution to the decay and τ_D is the unquenched fluorescence lifetime.

The apparent volume fraction of mixing $f'_m(t)$ is calculated from

$$f'_m(t) = \frac{B_1}{B_1 + B_2} \quad (2)$$

using the pre-exponential coefficients obtained from the fluorescence decay profiles fitted to equation (1). Two corrections have to be imposed on these data, one ($f'_m(0)$) due to energy transfer across the boundaries in the nascent films, and the other ($f'_m(\infty)$) due to possible incomplete mixing in the limit of infinite annealing time. These lead to

$$f_m(t) = \frac{f'_m(t) - f'_m(0)}{f'_m(\infty) - f'_m(0)} \quad (3)$$

We model $f'_m(\infty)$ by freeze drying a 1:1 mixture of Phe-labelled and An-labelled particles, dissolving the sample in THF and preparing a film by solvent casting. This was done separately for the four pairs of samples shown in *Table 1*, and $f'_m(\infty)$ values were always in the range 0.96–1.0.

The analysis given above is correct only if the value of P in equation (1) found from curve fitting is independent of the extent of mixing. From a theoretical point of view[17], it is the area under each $I_D(t)$ curve which is related to the quantum efficiency of emission, and from which the energy transfer quantum yields ϕ_{ET} should be calculated. If P is a constant, the area contributions of each term in equation (1) are proportional to the ratio of their prefactors. *Figure 4* shows that P values go through a minimum at early annealing times and increase only slowly to a constant value. This effect is more pronounced in samples rich in acid groups. Under these circumstances correct values of $f_m(t)$ must be calculated from the areas under the decay curves, i.e.

$$f_m(t) = \frac{\text{area}(t) - \text{area}(0)}{\text{area}(\infty) - \text{area}(0)} \quad (4)$$

where the areas are determined by integration after normalizing the decay curves at $t = 0$ ($B'_1 = B_1/(B_1 + B_2)$);

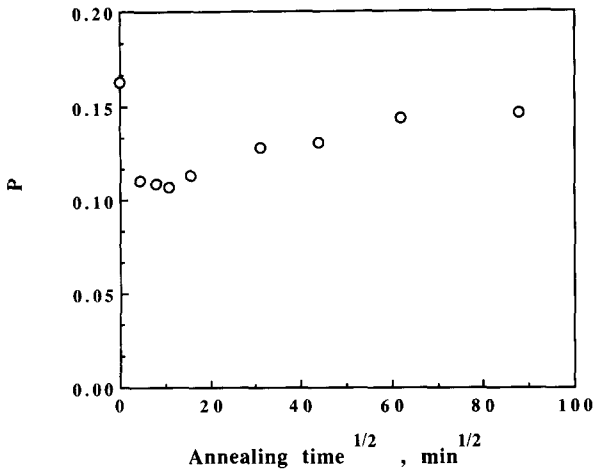

Figure 4 A plot of P *versus* $t^{1/2}$ for a sample of MA4 film annealed at 90°C. The P values were obtained by fitting fluorescence decay profiles to equation (1)

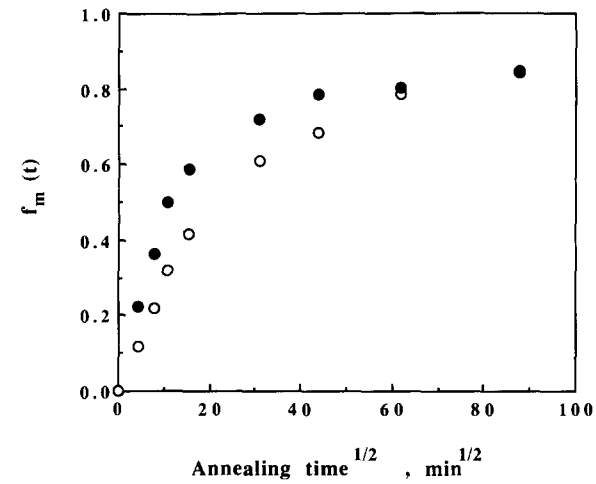

Figure 5 Plots of $f_m(t)$ *versus* $t^{1/2}$ for an MA4 film sample annealed at 90°C: (●) $f_m(t)$ calculated from prefactors, equations (2) and (3); (○) $f_m(t)$ calculated from areas, equation (4)

$B'_2 = B_2/(B_1 + B_2)$; $B'_1 + B'_2 = 1$)*. The effect is serious. One notes in *Figure 5* that $f_m(t)$ values calculated from $B_1/(B_1 + B_2)$ are significantly larger than those calculated from the areas, and would lead to diffusion coefficients that are too large.

Two final comments are in order about the analysis of the decay curves. The area method determines the extent of mixing through the quantum efficiency of energy transfer. Tirrell *et al.*[21] have pointed out that this approach has a general validity since it makes few assumptions about the interdiffusion process. The detailed shape of the $I_D(t)$ profile, on the other hand, is sensitive to the details of the donor–acceptor (Phe, An) pair distribution created by the interdiffusion process. This type of distribution is shown in cartoon form in *Figure 6*. The time dependence of the P parameter shown in *Figure 4* is a hopeful sign that in the future, more-sophisticated models can be developed and tested to extract information about the concentration profile resulting from interdiffusion at early reaction times.

Polymer interdiffusion

Polymer interdiffusion experiments were carried out on films prepared from MA0 (a 1:1 mixture of An-MA0 and Phe-MA0) using MA0 samples 'as prepared' and after ion exchange. The ion-exchanged latex underwent faster interdiffusion (*Figure 7*). Addition of small amounts

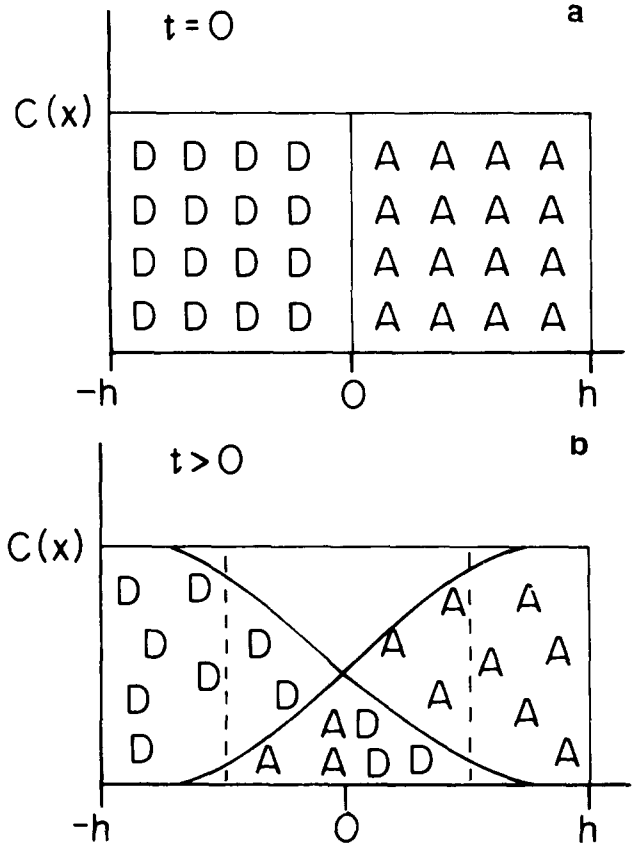

Figure 6 A cartoon representing (a) the initial sharp interface between donor-labelled (D) and acceptor-labelled (A) polymers, and (b) the evolution of the D/A pair concentration profile at some arbitrary time after the onset of diffusion

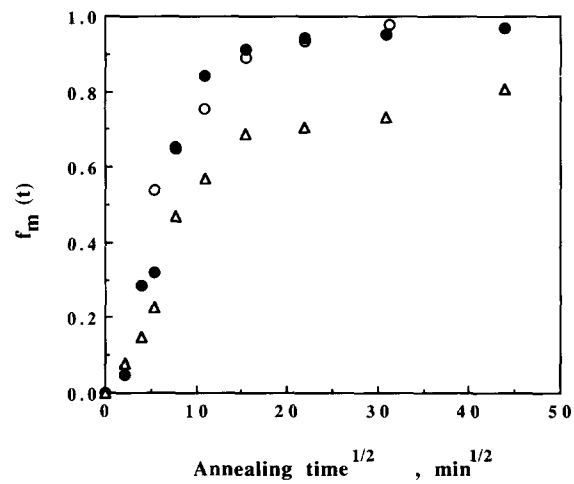

Figure 7 The effect of ion exchange on the rate of interdiffusion at 100°C in a latex film prepared from MA0: (△) film formed from latex as prepared; (○) film formed from latex cleaned by ion exchange; (●) film formed from ion-exchanged latex to which an amount of SDS equal to Q_s was added

* Data fitted to equation (1) can be integrated in closed form

$$\int_0^\infty I_D(t)\,dt = \tau_D\left[1 - \left(\frac{B_1 P}{B_1 + B_2}\right)\left(\frac{\pi^{1/2}}{2}\right)\mathrm{erfc}(P/2)\exp(P^2/4)\right]$$

of SDS (one SDS per surface OSO_3H group) had no noticeable effect on the interdiffusion rate. We ascribe the difference to neutralization of the OSO_3H groups to the sodium salt by the $NaHCO_3$ present in the reaction medium. The effect of counterions on polymer interdiffusion is an important topic which we hope to study in the near future.

Quantifying interdiffusion rates

To quantify the interdiffusion rate, we need to relate $f_m(t)$ values to polymer diffusion coefficients. This requires a model for the diffusion process. In previous work, we employed a Fickian diffusion model[22] and a spherical diffusion geometry to obtain D values[14–17]. Fickian diffusion models predict a linear dependence of $f_m(t)$ on $t^{1/2}$ for much of the interdiffusion process[17]. What we wish to do here is to draw some quantitative comparisons about the relative interdiffusion rates of MA0, MA2, MA4 and MA6. For these four film samples annealed at 90°C we plotted values of $f_m(t)$ *versus* $t^{1/2}$ (*Figure 8*). For comparison, we calculated the theoretical values $f_s(t)$, which describe the extent of mixing that would take place by a Fickian diffusion process characterized by a single D value. For details of this calculation, see ref. 17.

In *Figure 8* one observes that the rate of interdiffusion is significantly slower in latex films containing increasing numbers of carboxylic acid groups. One can appreciate this decrease in diffusivity in several ways. First one notes that the D values used to calculate $f_s(t)$ in *Figure 8* decrease from 6.5×10^{-16} cm^2 s^{-1} for MA0 to 0.9×10^{-16} cm^2 s^{-1} for MA6. Furthermore, the deviation from linearity of $f_m(t)$ *versus* $t^{1/2}$ occurs earlier for the samples richer in CO_2H groups. For these samples diffusion slows down more rapidly than one would expect for Fickian diffusion of a single substance.

We can use the data in *Figure 8* in conjunction with the spherical diffusion model to calculate cumulative D values as a function of annealing time. As in previous studies, these values decrease with increasing extent of interdiffusion. The effect is much more pronounced in the latex films containing larger amounts of acid groups. We emphasize this difference in *Figure 9* by plotting relative diffusion coefficients $D_{rel} = D_{MAx}/D_{MA0}$ against the acid group content of the latex for values of $f_m(t) = 0.2$, 0.4 and 0.6. It is clear that diffusivity decreases both with increasing acid content and extent of diffusion.

Interpreting the data

Our most important finding is that the presence of carboxylic acid groups at the particle surface does not prevent polymer interdiffusion. These groups do, however, retard this diffusion. Finding a proper explanation for this effect is the next major objective in developing an understanding of films prepared from carboxylated latex. This is not an easy task.

There are three factors which complicate quantitative data interpretation in these systems. Firstly, since the polymer molecular weights exceed the entanglement molecular weights, the diffusion process may not be Fickian. Secondly, the molecular weight polydispersity (M_w/M_n) introduces a distribution of diffusion coefficients. Thirdly, for the samples rich in carboxylic acid groups, there is significant compositional heterogeneity in the films.

We are unable at this point to provide any definitive insights into the Fickian or non-Fickian nature of the polymer diffusion, except to point out that these aspects

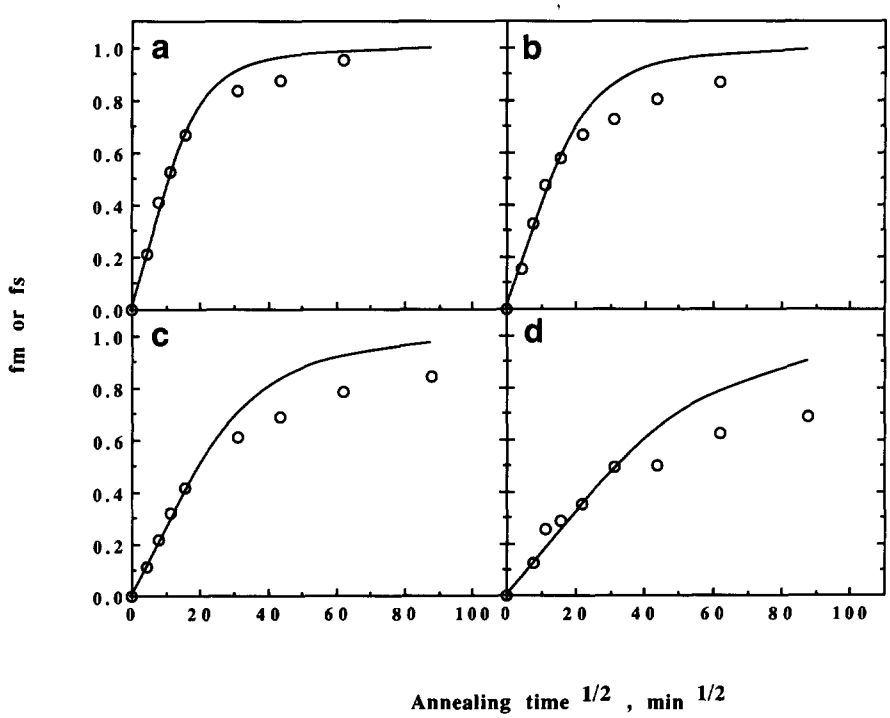

Figure 8 Plots of $f_m(t)$ calculated from fluorescence decay profiles via equation (4) *versus* $t^{1/2}$ for all four latex film samples. These values are compared to the theoretical values $f_s(t)$ computed by solving the Fickian spherical diffusion equation[17] in terms of a single diffusion coefficient D. Lines refer to $f_s(t)$; points refer to experimental $f_m(t)$ data. In calculating $f_s(t)$, the following D values were employed: (a) MA0, 6.5×10^{-16} cm^2 s^{-1}; (b) MA2, 6.0×10^{-16} cm^2 s^{-1}; (c) MA4, 2.7×10^{-16} cm^2 s^{-1}; (d) MA6, 0.90×10^{-16} cm^2 s^{-1}

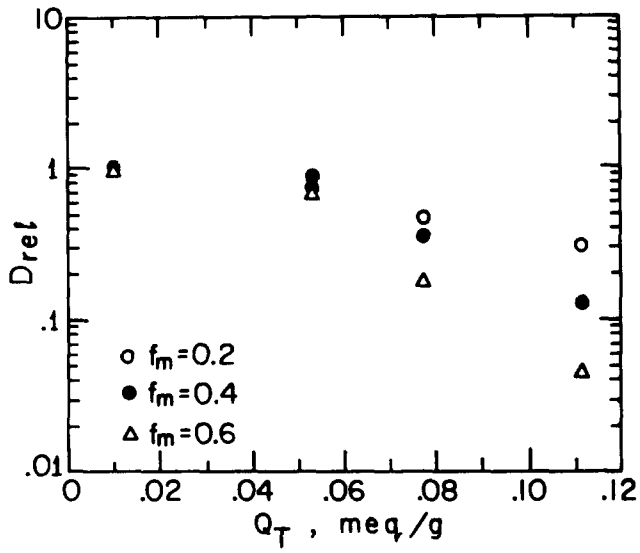

Figure 9 Plots of D_{rel} ($=D_{MAx}/D_{MA0}$) *versus* the total amount of surface acid groups Q_T for different extents of interdiffusion: (○) $f_m(t)=0.2$; (●) $f_m(t)=0.4$; (△) $f_m(t)=0.6$

should be similar in MA0 to those in the other samples. Here, future insights may come from a more sophisticated analysis of fluorescence decay profiles at the early stages of the interdiffusion process. In previous studies of simple PBMA latex films, we pointed out that preferential diffusion at early times of the lower molecular weight components of the latex film would lead in a natural way to the decrease in D with increasing annealing time.

The most interesting feature here is the role of the carboxylic acid groups in retarding interparticle diffusion. From the method of synthesis (monomer-starved addition, no obvious grafting), we expect the formation of a statistical BMA–MAA copolymer during the final stage of polymerization. For MA2 this copolymer should contain 2.0 mol% MAA. In each instance this copolymer comprises about 35 vol% of the total polymer. Phase segregation may also occur, especially in a core–shell material.

It is tempting to consider that an explanation for the reduction in diffusion rates is connected to the presence in the system of a blend of (labelled) PBMA homopolymer with a (similarly labelled) BMA–MAA copolymer. Our experiment detects interdiffusion of both homopolymer and carboxylated copolymer. The large values of $f_m(t)$ obtained indicate that interdiffusion of both species contributes to the mixing process.

Carboxylated copolymers normally have higher glass transition temperatures (T_g) than the corresponding homopolymers[23,24]. We can think of our system in terms of a shell of carboxylated copolymer surrounding a core of PBMA. The samples MA2, MA4 and MA6 contain, respectively, 1.26 wt%, 2.51 wt% and 5.78 wt% methacrylic acid in the third-stage polymer. Taking T_g values of 308 K for PBMA and 458 K for PMAA, we can estimate the T_g of the shell from the expression[25]

$$\frac{1}{T_g(\text{copolymer})}=\frac{w_1}{T_{g1}}+\frac{w_2}{T_{g2}} \qquad (5)$$

where w_1 and w_2 refer to the relative weights of the two components, and find 309 K for MA2, 311 K for MA4 and 314 K for MA6. Even though these changes are small, we expect that at a fixed temperature T the higher T_g polymers undergo diffusion at lower values of $(T-T_g)$. This has the effect of increasing the microscopic friction and decreasing the diffusion rate of such chains. This represents one explanation of the much more pronounced decrease in D with increasing carboxylic acid content at $f_m=0.6$ than at earlier extents of interdiffusion.

On the other hand, Green and Doyle[26] and Klein *et al.*[27] have shown that the interdiffusion of miscible polymers near the critical temperature is retarded ('thermodynamic slowing down') and that the extent of interdiffusion of immiscible polymers is limited. The χ parameter for mixtures of PBMA homopolymer with BMA–MAA copolymers is likely to be positive. This also might explain the decrease in D with increasing extent of interdiffusion.

Our results indicate that significant interdiffusion occurs early in the annealing process, and that the interdiffusion process is dominated by the fastest diffusing species in the sample. These are likely to be the polymers of lowest molecular weight and lowest carboxylic acid content. At longer annealing times, slow-moving polymers make increasing contributions to the energy transfer signal.

A very different type of behaviour has been reported recently for poly(styrene-*co*-butyl acrylate) latex surrounded by a thin shell very rich in acrylic acid[28]. Here, the thin layer of acid-rich polymer forms an interconnecting membrane as the latex film forms. The membrane was detected by neutron scattering following exposure of the film to D_2O. This membrane has a sufficiently high T_g when dry to act as a barrier, and appears to block interdiffusion completely. Only upon raising the temperature of the film above the T_g of the acid-rich polymer did the membrane break up into droplets. This process should bring the core polymers of adjacent latexes in the film into intimate contact and thus permit interdiffusion to occur.

The challenge now is to understand the various factors that control interdiffusion in latex films containing polar material at the interparticle boundary. There are some obvious experiments for us to carry out on films formed from the system of latex particles we have described here, such as examining the effects of temperature and acid group neutralization on interdiffusion. The results of these experiments will be reported in due course. One approach that seems particularly attractive for future work is the idea of labelling selectively the second-stage or third-stage polymer during the latex synthesis. In this way it should be possible to identify which type of polymer contributes at various times to the interdiffusion process.

ACKNOWLEDGEMENTS

The authors thank ICI Ltd, ICI Canada and the Glidden Co. for funding through the ICI–SRF programme, as well as NSERC Canada for its support of this research.

REFERENCES

1 Wool, R. P., Yuan, B.-L. and McGarel, O. J. *Polym. Eng. Sci.* 1989, **16**, 204
2 Kausch, H. H. and Tirrell, M. *Annu. Rev. Mater. Sci.* 1989, **19**, 341
3 Yoo, J. N., Sperling, L. H., Glinka, C. J. and Klein, A. *Macromolecules* 1990, **23**, 3962
4 Kanig, G. and Neff, H. *Colloid Polym. Sci.* 1975, **253**, 29
5 Kanig, G. *Colloid Polym. Sci.* 1978, **256**, 1052

6 Richard, J. *Polymer* 1992, **33**, 562
7 Richard, J., Mignang, C. and Wong, K. *Polym. Int.* 1992, **33**, 4164
8 Joanicot, M., Wong, K., Maquet, J., Chevalier, Y., Pickot, C., Graillat, C., Lindner, P., Rios, L. and Cabane, B. *Prog. Colloid Polym. Sci.* 1990, **81**, 175
9 Chevalier, Y., Pichot, C., Graillat, J., Joanicot, M., Wong, K., Lindner, P. and Cabane, B. *Colloid Polym. Sci.* 1992, **270**, 806
10 Hahn, K., Ley, G., Schuller, H. and Oberthur, R. *Colloid Polym. Sci.* 1986, **64**, 1029
11 Hahn, K., Ley, G., Schuller, H. and Oberthur, R. *Colloid Polym. Sci.* 1988, **66**, 631
12 Linne, M. A., Klein, A. and Sperling, L. H. *J. Macromol. Sci. Phys. B.* 1988, **27**, 181
13 Linne, M. A., Klein, A. and Sperling, L. H. *J. Macromol. Sci. Phys. B* 1988, **27**, 217
14 Zhao, C.-L., Wang, Y., Hruska, Z. and Winnik, M. A. *Macromolecules* 1990, **23**, 4082
15 Winnik, M. A., Wang, Y. and Haley, F. *J. Coat. Technol.* 1992, **64**, 51
16 Winnik, M. A., Wang, Y. and Zhao, C.-L. in 'Photochemical Processes in Organized Molecular Systems' (Ed. K. Honda), Elsevier, Amsterdam, 1991, p. 275
17 Wang, Y., Zhao, C.-L. and Winnik, M. A. *J. Chem. Phys.* 1991, **95**, 2143
18 Everett, D. H., Gültepe, X. and Wilkinson, M. C. *J. Colloid Interface Sci.* 1979, **71**, 336
19 Rymdén, J. *J. Colloid Interface Sci.* 1988, **124**, 396
20 Bangs, L. B. 'Uniform Latex Particles', Seradyn, Indianapolis, 1984
21 Tirrell, M., Adolf, D. and Prager, S. *Springer Lecture Notes Appl. Math.* 1984, **37**, 1063
22 Crank, J. 'The Mathematics of Diffusion', Clarendon Press, Oxford, 1975
23 Eisenberg, A. *Macromolecules* 1976, **4**, 125
24 Matsuura, H. and Eisenberg, A. *J. Polym. Sci., Polym. Phys. Edn* 1976, **14**, 1201
25 Rodriguez, F. 'Principles of Polymer Systems', 2nd Edn, McGraw Hill, New York, 1982, p. 39
26 Green, P. F. and Doyle, B. L. *Phys. Rev. Lett.* 1986, **57**, 2407
27 Steiner, U., Krausch, G., Schatz, G. and Klein, J. *Phys. Rev. Lett.* 1990, **64**, 1119
28 Joanicot, M., Wong, K., Richard, J., Maquet, J. and Cabane, B. *Macromolecules* 1993, **26**, 3168